

Learning from Acquisition: Metadata-driven Multimodal Pre-training for Cardiac MRI

Xueyi Fu¹, Liwei Hu², Zi Wang^{2✉}, and Guang Yang^{2,3,4,5✉}

- ¹ Department of Surgery & Cancer, Imperial College London, London, UK
² Bioengineering Department and Imperial-X, Imperial College London, London, UK
³ National Heart and Lung Institute, Imperial College London, London, UK
⁴ Cardiovascular Research Centre, Royal Brompton Hospital, London, UK
⁵ School of Biomedical Engineering & Imaging Sciences, King's College London, London, UK

✉ {zi.wang,g.yang}@imperial.ac.uk

Abstract. Cardiac magnetic resonance imaging (CMR) routinely records structured acquisition metadata, yet most CMR foundation models rely primarily on image-only pre-training and leave this naturally available source of weak semantic supervision largely underexplored. We propose MetaCLIP-CMR, a metadata-driven framework based on Contrastive Language-Image Pre-training (CLIP), which converts imaging modality, anatomical view, scanner vendor, field strength, and scanner model into textual supervision for CMR representation learning. The pretrained image encoder is evaluated on imaging modality classification, cine view classification, and cardiac segmentation. MetaCLIP-CMR achieves 86.8% modality accuracy and 86.5% cine view accuracy, clearly outperforming ImageNet and masked reconstruction initialisations. For downstream cardiac segmentation, MetaCLIP-CMR consistently obtains the highest Dice score across the evaluated ACDC and M&Ms cine short-axis (SAX) settings under both full-data and 20% fine-tuning regimes. Compared with recent image-focused large-scale CMR pre-training models, MetaCLIP-CMR achieves comparable ACDC segmentation performance, while requiring less than 1% of their pre-training image scale. These results suggest that metadata learning offers a natural and easy-to-use strategy for transforming routinely recorded acquisition information into effective supervision for foundation-level CMR representation learning, highlighting the promise of metadata-driven multimodal pre-training.

Keywords: Cardiac MRI · Foundation Models · CLIP · Metadata · Multimodal Learning

1 Introduction

Cardiac magnetic resonance imaging (CMR) provides complementary anatomical, functional, and tissue-characterisation information across cine, late gadolinium enhancement (LGE), mapping, flow, and other acquisition sequences [7, 9, 15]. This diversity also introduces substantial variation in image appearance across modalities, anatomical views, scanner vendors, and field strengths.

Recent medical and CMR foundation models have mainly relied on image-only self-supervised learning, including masked image modelling, contrastive learning, and self-distillation [4, 10, 13]. In CMR, the DINO-based model [6] learns visual representations from large-scale heterogeneous CMR data, while CineMA [3] applies masked image modelling to large-scale cine CMR. These studies show that CMR-specific pre-training can support downstream segmentation and classification [6, 17]. However, their supervision is derived primarily from image appearance and does not explicitly incorporate acquisition-level information such as imaging modality, anatomical view, vendor, or field strength.

Vision–language models such as CLIP [11] introduce semantic supervision by aligning images with text. Medical variants have further demonstrated the value of image–text pre-training for transferable medical representations [16, 18]. Their application to CMR is limited by the availability of paired clinical reports or manually curated textual annotations. In contrast, acquisition metadata are routinely recorded during scanning and provide structured information without additional manual annotation.

We therefore propose MetaCLIP-CMR, a metadata-driven image–text pre-training framework that converts imaging modality, anatomical view, scanner vendor, field strength, and scanner model into textual descriptions. The pre-trained image encoder is evaluated on modality classification, cine view classification, and cine short-axis segmentation. The classification tasks assess whether metadata-defined concepts are transferred to the image representation, while segmentation evaluates transfer to a pixel-level task not directly specified by the text. Beyond internal comparisons with ImageNet and masked reconstruction initialisation, we further contextualise MetaCLIP-CMR against recent image-focused CMR pre-training models to assess the efficiency of metadata-driven pre-training relative to large-scale image-only representation learning.

Our main contributions are:

- We introduce a metadata-driven CMR image–text pre-training framework that transforms routinely recorded acquisition information into natural, structured, and easy-to-use weak semantic supervision, without requiring manually paired clinical reports or curated text annotations.
- We demonstrate that MetaCLIP-CMR learns modality- and view-aware representations that transfer consistently to cine short-axis segmentation, outperforming ImageNet and masked reconstruction baselines in imaging classification and cardiac segmentation.
- Compared with recent image-focused large-scale CMR pre-training models, MetaCLIP-CMR reaches comparable segmentation performance while using less than 1% of their pre-training image scale, highlighting the potential of metadata learning for efficient CMR representation pre-training.

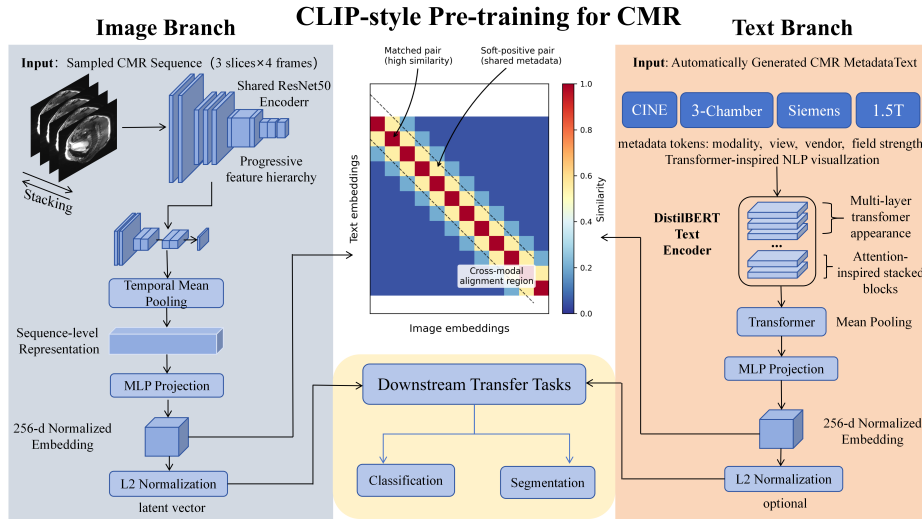


Fig. 1. Overview of MetaCLIP-CMR. Image sequences and metadata-derived text are projected into a shared 256-dimensional space and aligned using the proposed soft-label contrastive loss.

2 Method

2.1 Overview

MetaCLIP-CMR aligns CMR sequences with metadata-derived text in a shared embedding space. As shown in Fig. 1, the model contains image and text encoders with projection heads trained using a metadata-aware contrastive loss. After pre-training, only the image encoder is retained.

2.2 Preprocessing and Metadata Text

Data preprocessing. Raw k-space data from MMCMR-427K database [14] are reconstructed offline using sum-of-squares (SOS) reconstruction and stored as 2D .npy slices. Each slice is z-score normalised and resized to 224×224 pixels. During pre-training, we sample $N_s = 3$ slices and up to $N_f = 4$ frames per sequence, yielding up to 12 images. If fewer than four frames are available, all available frames are used without repetition. Augmentation includes random horizontal flipping, rotation ($\pm 10^\circ$), translation of up to 10%, and Gaussian noise ($\sigma \in [0.005, 0.05]$), with consistent spatial transformations across images from the same sequence.

Metadata text generation. Structured acquisition metadata are converted into text using predefined templates (Fig. 2). For sequence i ,

$$t_i = \mathcal{T}(a_{i1}, \dots, a_{iK}), \quad (1)$$

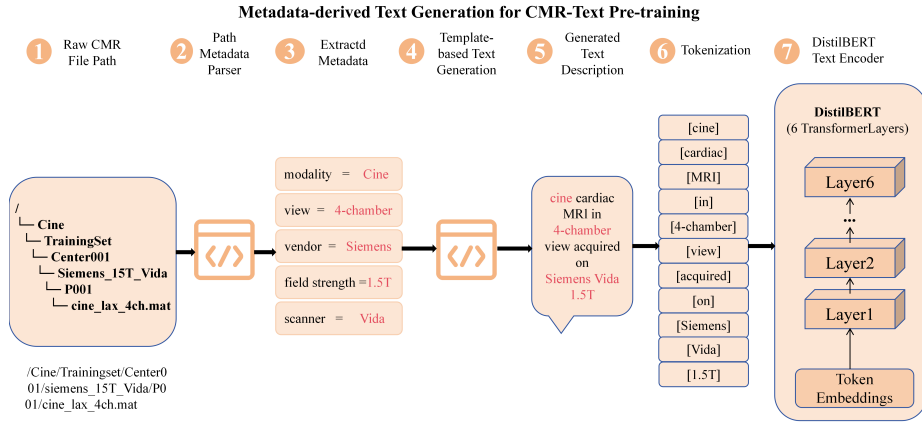


Fig. 2. Metadata-derived text generation from CMR modality, anatomical view, scanner vendor, field strength, and scanner model.

where the attributes include CMR modality, anatomical view, scanner vendor, field strength, and scanner model. An example is: “*cine cardiac MRI in short-axis view acquired on a 3.0T scanner*”. The descriptions are generated automatically from metadata parsed from the dataset organisation, without manual annotation.

2.3 Multimodal Pre-training

The image encoder f_θ is a single-channel ResNet-50 that processes each sampled image independently. Let x_{it} denote the t -th sampled image from sequence i . The corresponding image feature is

$$h_{it} = f_\theta(x_{it}) \in \mathbb{R}^{2048}. \quad (2)$$

The features from the T_i sampled images are mean-pooled to obtain a sequence-level representation:

$$\bar{h}_i = \frac{1}{T_i} \sum_{t=1}^{T_i} h_{it}. \quad (3)$$

The text encoder g_ϕ is DistilBERT [12]. Image and text representations are projected into a shared 256-dimensional space by W_v and W_u , respectively, and L2-normalised:

$$v_i = \frac{W_v \bar{h}_i}{\|W_v \bar{h}_i\|}, \quad u_i = \frac{W_u g_\phi(t_i)}{\|W_u g_\phi(t_i)\|}. \quad (4)$$

Following CLIP [11], the image-text similarity matrix is

$$S_{ij} = v_i^\top u_j. \quad (5)$$

Standard CLIP treats only the matched image–text pair as positive and all other pairs in the batch as negatives. In CMR, however, different sequences may share acquisition semantics such as imaging modality or anatomical view. We therefore assign weaker positive weights to non-matched samples sharing these attributes.

To account for acquisition-level similarities between CMR sequences, we replace the one-hot CLIP targets with metadata-aware soft targets:

$$\tilde{Q}_{ij} = \mathbb{I}(i = j) + \alpha \mathbb{I}(i \neq j, m_i = m_j) + \beta \mathbb{I}(i \neq j, r_i = r_j), \quad (6)$$

where m_i and r_i denote the modality and anatomical view of sequence i . The exact image–text pair receives weight 1, while non-matched samples sharing the same modality or view receive weaker positive weights $\alpha = \beta = 0.05$. If both attributes are shared, the two contributions are added. The view term is applied only when valid view annotations are available.

The targets are normalised along each row:

$$Q_{ij} = \frac{\tilde{Q}_{ij}}{\sum_{k=1}^B \tilde{Q}_{ik}}. \quad (7)$$

Thus, each row defines a probability distribution over the candidate samples in a batch of size B .

The bidirectional soft-label contrastive loss is

$$\mathcal{L} = \frac{1}{2} [\text{SCE}(Q, S/\tau) + \text{SCE}(Q, S^\top/\tau)], \quad (8)$$

where τ is a learnable temperature and

$$\text{SCE}(Q, Z) = -\frac{1}{B} \sum_{i=1}^B \sum_{j=1}^B Q_{ij} \log \frac{\exp(Z_{ij})}{\sum_{k=1}^B \exp(Z_{ik})}. \quad (9)$$

The row-wise normalisation corresponds to selecting texts for each image in the image-to-text direction and images for each text in the text-to-image direction.

For image-only comparison, we train a ResNet-50 masked reconstruction baseline following the general masked image modelling paradigm [4]. A lightweight decoder reconstructs masked regions and is discarded after pre-training.

2.4 Downstream Transfer

The pretrained image encoder is evaluated on CMR modality classification, cine view classification, and cardiac segmentation.

We use a two-stage linear probing and fine-tuning protocol (Probe+FT). During the probe stage, the image encoder is frozen and only the task-specific head or decoder is trained. The encoder is then unfrozen and the full network is fine-tuned using a smaller learning rate for the encoder.

Table 1. Datasets used for pre-training and downstream evaluation. Our used MMCMR-427K subset contains 10 CMR modalities from five vendors and 1.5T/3.0T systems.

| Dataset | Task | Train / Test |
|------------|--------------------------|-------------------------|
| MMCMR-427K | Pre-training | 4,672 / 2,385 sequences |
| | Modality classification | 4,672 / 1,914 sequences |
| | Cine view classification | 4,672 / 576 sequences |
| ACDC | Segmentation | 100 / 50 cases |
| M&Ms | Segmentation | 150 / 136 cases |

3 Experiments and Results

3.1 Datasets and Implementation

In this study, We use a subset of the original MMCMR-427K database [14]. The source database contains 427,465 paired k-space samples. The subset used in this work contains 7,057 CMR sequences spanning 10 CMR modalities, five vendors, and 1.5T/3.0T systems, with 4,672 used for pre-training and 2,385 held out (Table 1). Held-out MMCMR-427K sequences are used for CMR modality and cine view classification. ACDC [1] and M&Ms [2] are used for cine short-axis segmentation. The evaluation sets remain unchanged, and the same reduced-data subsets are used for all initialisation methods.

MetaCLIP-CMR uses a ResNet-50 image encoder [5] and a DistilBERT text encoder [12], with both branches projected into a 256-dimensional embedding space. Pre-training is performed for 30 epochs using AdamW [8]. We compare MetaCLIP-CMR with ImageNet initialisation and image-only masked reconstruction. Classification is evaluated by accuracy and segmentation by case-level 3D Dice.

3.2 Metadata-aligned Classification

To assess whether metadata-derived supervision is transferred to the image representation, we evaluate CMR modality and cine view classification, as both attributes are explicitly encoded in the pre-training text.

MetaCLIP-CMR achieves the highest accuracy in both tasks (Table 2). Its strong probe performance, together with the small additional gain after fine-tuning, indicates that modality- and view-level semantics are already linearly accessible from the frozen representation.

This suggests that metadata-driven pre-training does not merely improve downstream classification accuracy, but organises the image embedding space around clinically meaningful acquisition concepts. These results provide direct evidence that routinely recorded acquisition metadata can act as effective semantic supervision for learning acquisition-aware CMR representations.

Table 2. CMR modality and cine view classification accuracy. Probe denotes frozen-encoder evaluation, and Probe+FT denotes subsequent end-to-end fine-tuning.

| Method | Mod. Probe | Mod. Probe+FT | View Probe | View Probe+FT |
|---------------|--------------|---------------|--------------|---------------|
| ImageNet | 0.686 | 0.751 | 0.740 | 0.793 |
| Masked recon. | 0.658 | 0.729 | 0.655 | 0.682 |
| MetaCLIP-CMR | 0.864 | 0.868 | 0.830 | 0.865 |

3.3 Transfer to Cine SAX Segmentation

To assess transfer beyond metadata-aligned classification, we evaluate cine short-axis segmentation on ACDC and M&Ms using the same Probe+FT protocol for all pre-training methods.

MetaCLIP-CMR obtains the highest Dice across all four evaluated settings (Table 3) and produces the most accurate visual segmentation among the compared pre-training methods (Figure 3). The improvement is particularly evident in the 20% ACDC and full-data M&Ms settings, suggesting that metadata-driven pre-training can provide useful transferable representations even for pixel-level tasks that are not directly specified by the pre-training text. Figure 3 shows representative ACDC and M&Ms results. The arrows indicate local contour errors in the ImageNet and masked reconstruction predictions.

Together with the classification results, these findings indicate that acquisition metadata provide a natural and effective supervision signal for learning CMR representations that transfer across both acquisition-aware and anatomy-oriented downstream tasks.

Table 3. Case-level mean Dice for cine SAX segmentation. The 100% settings use 100 ACDC and 150 M&Ms training cases, while the 20% settings use 20 and 30 cases, respectively.

| Method | ACDC 100% | ACDC 20% | M&Ms 100% | M&Ms 20% |
|---------------|---------------|---------------|---------------|---------------|
| ImageNet | 0.8997 | 0.8642 | 0.8260 | 0.7965 |
| Masked recon. | 0.8994 | 0.8635 | 0.8300 | 0.7966 |
| MetaCLIP-CMR | 0.9021 | 0.8795 | 0.8368 | 0.8008 |

3.4 Comparison with Large-scale CMR Pre-training Models

Here, we further contextualise MetaCLIP-CMR against recent image-focused CMR large-scale pre-training models on ACDC segmentation. Although differences in data, architectures, and evaluation protocols prevent a strictly controlled comparison, the reported results provide a useful reference for downstream performance.

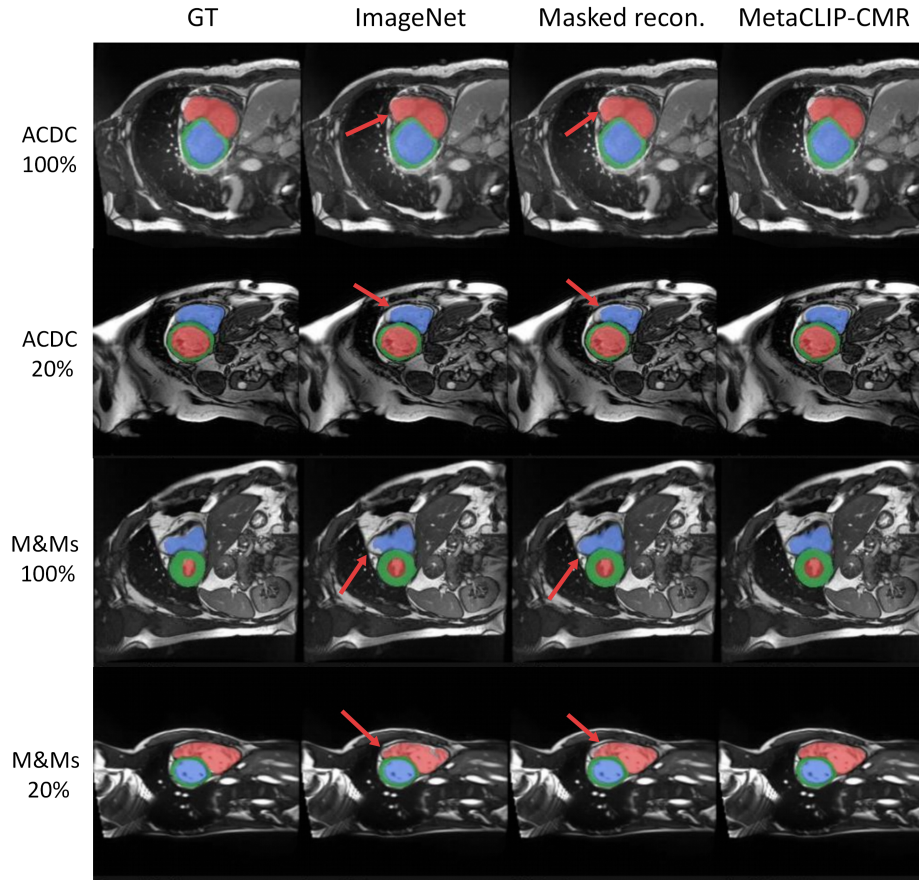


Fig. 3. Representative cine SAX segmentation results on ACDC and M&Ms under full-data and 20% settings. RV, myocardium (MYO), and LV are shown in red, green, and blue, respectively.

MetaCLIP-CMR achieves a mean ACDC Dice of 0.902, close to the DINO-based CMR model (0.906) [6] and CineMA (0.909) [3]. The latter models were pretrained on approximately 36 million CMR images [6] and more than 15 million cine CMR images [3], respectively, whereas MetaCLIP-CMR uses approximately 0.2 million but more diverse CMR images [14]. This suggests that metadata-driven multimodal pre-training can approach the performance of much larger image-focused CMR models with less than 1% of their pre-training image scale.

4 Conclusion

We presented MetaCLIP-CMR, a metadata-driven image–text pre-training framework. By converting routinely recorded acquisition information into textual de-

scriptions, MetaCLIP-CMR turns a naturally available and easy-to-use source of weak semantic information into supervision for CMR representation learning.

Future work will extend metadata-driven pre-training with richer protocol information and temporal modelling across larger multi-centre, multi-vendor, and multi-disease CMR cohorts, while exploring broader downstream tasks such as cardiac phenotyping, disease classification, image quality control, and cross-modality retrieval.

References

1. Bernard, O., Lalande, A., Zotti, C., Cervenansky, F., Yang, X., Heng, P.A., Cetin, I., Lekadir, K., Camara, O., Gonzalez Ballester, M.A., Sanroma, G., Napel, S., Petersen, S., Tziritas, G., Grinias, E., Khened, M., Kollerathu, V.A., Krishnamurthi, G., Rohe, M.M., Pennec, X., Sermesant, M., Isensee, F., Jager, P., Maier-Hein, K.H., Full, P.M., Wolf, I., Engelhardt, S., Baumgartner, C.F., Koch, L.M., Wolterink, J.M., Isgum, I., Jang, Y., Hong, Y., Patravali, J., Jain, S., Humbert, O., Jodoin, P.M.: Deep learning techniques for automatic mri cardiac multi-structures segmentation and diagnosis: Is the problem solved? *IEEE Transactions on Medical Imaging* **37**(11), 2514–2525 (nov 2018). <https://doi.org/10.1109/TMI.2018.2837502>
2. Campello, V.M., Gkontra, P., Izquierdo, C., Martin-Isla, C., Sojoudi, A., Full, P.M., Maier-Hein, K., Zhang, Y., He, Z., Ma, J., Parreno, M., Albiol, A., Kong, F., Shadden, S.C., Acero, J.C., Sundaresan, V., Saber, M., Elattar, M., Li, H., Menze, B., Khader, F., Haarburger, C., Scannell, C.M., Veta, M., Carscadden, A., Punithakumar, K., Liu, X., Tsaftaris, S.A., Huang, X., Yang, X., Li, L., Zhuang, X., Vilades, D., Descalzo, M.L., Guala, A., Mura, L., Friedrich, M.G., Garg, R., Lebel, J., Henriques, R., Karakas, M.O., Cavus, O., Petersen, S.E., Escalera, S., Segui, S., Rodriguez-Palomares, J.F., Lekadir, K.: Multi-centre, multi-vendor and multi-disease cardiac segmentation: The m&ms challenge. *IEEE Transactions on Medical Imaging* **40**(12), 3543–3554 (2021). <https://doi.org/10.1109/TMI.2021.3090082>
3. Fu, Y., Bai, W., Yi, W., Manisty, C., Bhuvra, A.N., Treibel, T.A., Moon, J.C., Clarkson, M.J., Davies, R.H., Hu, Y.: Development and validation of a versatile foundation model for cine cardiac magnetic resonance image analysis. *Communications Medicine* (05 2026). <https://doi.org/10.1038/s43856-026-01636-0>
4. He, K., Chen, X., Xie, S., Li, Y., Dollár, P., Girshick, R.: Masked autoencoders are scalable vision learners (2021), <https://arxiv.org/abs/2111.06377>
5. He, K., Zhang, X., Ren, S., Sun, J.: Deep residual learning for image recognition (2015), <https://arxiv.org/abs/1512.03385>
6. Jacob, A.J., Borgohain, I., Chitiboi, T., Sharma, P., Comaniciu, D., Rueckert, D.: Towards a cardiovascular magnetic resonance foundation model for multi-task cardiac image analysis. *Journal of Cardiovascular Magnetic Resonance* **27**(2), 101967 (2025). <https://doi.org/10.1016/j.jocmr.2025.101967>
7. Li, L., Ding, W., Huang, L., Zhuang, X., Grau, V.: Multi-modality cardiac image computing: A survey. *Medical Image Analysis* **88**, 102869 (2023). <https://doi.org/10.1016/j.media.2023.102869>
8. Loshchilov, I., Hutter, F.: Decoupled weight decay regularization (2019), <https://arxiv.org/abs/1711.05101>
9. Morales, M.A., Manning, W.J., Nezafat, R.: Present and future innovations in ai and cardiac mri. *Radiology* **310**(1), e231269 (2024). <https://doi.org/10.1148/radiol.231269>
10. Paschali, M., Chen, Z., Blankemeier, L., Varma, M., Youssef, A., Bluethgen, C., Langlotz, C., Gatidis, S., Chaudhari, A.: Foundation models in radiology: What, how, why, and why not. *Radiology* **314**(2), e240597 (2025). <https://doi.org/10.1148/radiol.240597>, pMID: 39903075
11. Radford, A., Kim, J.W., Hallacy, C., Ramesh, A., Goh, G., Agarwal, S., Sastry, G., Askell, A., Mishkin, P., Clark, J., Krueger, G., Sutskever, I.: Learning transferable visual models from natural language supervision (2021), <https://arxiv.org/abs/2103.00020>

12. Sanh, V., Debut, L., Chaumond, J., Wolf, T.: Distilbert, a distilled version of bert: smaller, faster, cheaper and lighter (2020), <https://arxiv.org/abs/1910.01108>
13. Sun, Y., Wang, L., Li, G., Lin, W., Wang, L.: A foundation model for enhancing magnetic resonance images and downstream segmentation, registration and diagnostic tasks. *Nature Biomedical Engineering* **9**(4), 521–538 (2025). <https://doi.org/10.1038/s41551-024-01283-7>
14. Wang, Z., Huang, M., Shi, Z., Hu, H., Lan, L., Zhang, H., Li, Y., Hu, X., Lu, Q., Zhu, Z., Yao, Q., Dai, Y., Wang, F., Wu, Y., Lyu, J., Gao, Q., Xu, G., Zhang, Z., Zhang, H., Li, Q., Wang, G., He, T., Lan, L., Li, S., Xue, L., Sun, M., Lyu, Y., Hu, J., Zhu, J., Ahmad, R., Bu, Z., Qian, X., Cai, G., Cao, R., Cai, W., Xu, C., Ren, Y., Yu, F., Ma, S., Xu, Z., Chen, X., Hua, S., Kim, D., Zhang, Y., Ouyang, C., Bai, W., Qin, J., Yang, Y., Rueckert, D., Wang, H., Tao, Q., Prieto, C., Markl, M., Young, A., Wu, L., Wang, S., Qin, C., Zeng, M., Hu, X., Xu, H., Qu, X., Li, H., Yang, G., Wang, C.: Enabling ultra-fast cardiovascular imaging across heterogeneous clinical environments with a generalist foundation model and multimodal database (2025), <https://arxiv.org/abs/2512.21652>
15. Wang, Z., Wang, F., Qin, C., Lyu, J., Ouyang, C., Wang, S., Li, Y., Yu, M., Zhang, H., Guo, K., Shi, Z., Li, Q., Xu, Z., Zhang, Y., Li, H., Hua, S., Chen, B., Sun, L., Sun, M., Li, Q., Chu, Y.H., Bai, W., Qin, J., Zhuang, X., Prieto, C., Young, A., Markl, M., Wang, H., Wu, L.M., Yang, G., Qu, X., Wang, C.: Cmrrecon2024: A multimodality, multiview k-space dataset boosting universal machine learning for accelerated cardiac mri. *Radiology: Artificial Intelligence* **7**(2), e240443 (2025). <https://doi.org/10.1148/ryai.240443>, PMID: 39878610
16. Zhang, S., Xu, Y., Usuyama, N., Xu, H., Bagga, J., Tinn, R., Preston, S., Rao, R., Wei, M., Valluri, N., Wong, C., Tupini, A., Wang, Y., Mazzola, M., Shukla, S., Liden, L., Gao, J., Crabtree, A., Piening, B., Bifulco, C., Lungren, M.P., Naumann, T., Wang, S., Poon, H.: Biomedclip: a multimodal biomedical foundation model pretrained from fifteen million scientific image-text pairs (2025), <https://arxiv.org/abs/2303.00915>
17. Zhang, Y., Hager, P., Liu, C., Shit, S., Chen, C., Rueckert, D., Pan, J.: Towards cardiac mri foundation models: Comprehensive visual-tabular representations for whole-heart assessment and beyond. *Medical Image Analysis* **106**, 103756 (2025). <https://doi.org/10.1016/j.media.2025.103756>
18. Zhao, Z., Liu, Y., Wu, H., Wang, M., Li, Y., Wang, S., Teng, L., Liu, D., Cui, Z., Wang, Q., Shen, D.: Clip in medical imaging: A survey. *Medical Image Analysis* **102**, 103551 (2025). <https://doi.org/10.1016/j.media.2025.103551>